nature climate change

Article

https://doi.org/10.1038/s41558-022-01537-9

Adaptive emission reduction approach to reach any global warming target

Received: 6 August 2021

Accepted: 19 October 2022

Published online: 01 December 2022

Check for updates

Jens Terhaar [1,2] ✉, Thomas L. Frölicher [1,2], Mathias T. Aschwanden[1,2], Pierre Friedlingstein [3,4] & Fortunat Joos [1,2]

The parties of the Paris Agreement agreed to keep global warming well below 2 °C and pursue efforts to limit it to 1.5 °C. A global stocktake is instituted to assess the necessary emissions reductions every 5 years. Here we propose an adaptive approach to successively quantify global emissions reductions that allow reaching a temperature target within ±0.2 °C, solely based on regularly updated observations of past temperatures, radiative forcing and emissions statistics, and not on climate model projections. Testing this approach using an Earth system model of intermediate complexity demonstrates that defined targets can be reached following a smooth emissions pathway. Its adaptive nature makes the approach robust against inherent uncertainties in observational records, climate sensitivity, effectiveness of emissions reduction implementations and the metric to estimate CO_2 equivalent emissions. This approach allows developing emission trajectories for CO_2, CH_4, N_2O and other agents that iteratively adapt to meet a chosen temperature target.

Human-made emissions of greenhouse gases (GHG) and other radiative forcing agents have led to global warming of around 1.2 °C by 2020[1], with already observable negative impacts on the world's climate and ecosystems[2,3]. To limit the impact from further warming[4,5], 191 countries signed the Paris agreement to 'keep global warming well below 2 °C and to pursue efforts to limit it to 1.5 °C' by reducing GHG emissions[6]. As a central part of the agreement, a regular 5 yr stocktake process was instituted to assess collective progress in reducing emissions over the previous 5 yr period and to reassess the necessary global emissions reductions for the following 5 yr and beyond. Each signatory country provides its nationally determined contributions (NDCs) to the globally necessary GHG emissions reductions.

These necessary reductions to reach a chosen temperature target are often derived using the concept of a remaining emissions budget (REB)[2,7–9]. Such a REB quantifies the total allowed emissions that can still be emitted from the present-day onwards before a temperature target is reached. In the past, REBs usually only included CO_2[8–12]. Non-CO_2 forcing agents were generally included as prescribed scenario-dependent climate forcing, bringing an additional uncertainty into the remaining carbon budget[8–13]. To consider emissions of different radiative forcing agents and precursors in one budget, the concepts of Global Warming Potential (GWP)[14] and CO_2-forcing equivalent (CO_2-fe) emissions[7,15,16] can be used. The GWP for a time horizon of 100 yr (GWP-100) is the metric applied by the parties of the Paris Agreement, although GWP-100 CO_2 equivalent emissions from different gases do not result in identical forcing trajectories and climate impacts[7,15,17–19] and other metrics can be additionally used for reporting[20]. CO_2-fe emissions are defined as the amount of CO_2 emissions that would cause the same radiative forcing trajectory as emissions from a non-CO_2 agent (for example, methane). Thus, the CO_2-fe metric is best suited to compare emissions from different agents in the context of forcing and temperature stabilization pathways. However, even when non-CO_2 emissions are transferred to CO_2-fe emissions and added to the total REB, and not treated as an additional uncertainty of the remaining carbon emissions budget, estimations of the REB in 2020 that allows reaching the 1.5 °C temperature target still vary by a factor of more than two (130–300 Pg C)[7,21].

This range mainly stems from uncertainties in the global temperature response to changes in radiative forcing agents and

[1]Climate and Environmental Physics, Physics Institute, University of Bern, Bern, Switzerland. [2]Oeschger Centre for Climate Change Research, University of Bern, Bern, Switzerland. [3]College of Engineering, Mathematics and Physical Sciences, University of Exeter, Exeter, UK. [4]Laboratoire de Météorologie Dynamique, Institut Pierre-Simon Laplace, CNRS-ENS-UPMC-X, Paris, France. ✉e-mail: jens.terhaar@unibe.ch

https://doi.org/10.1038/s41558-022-01537-9

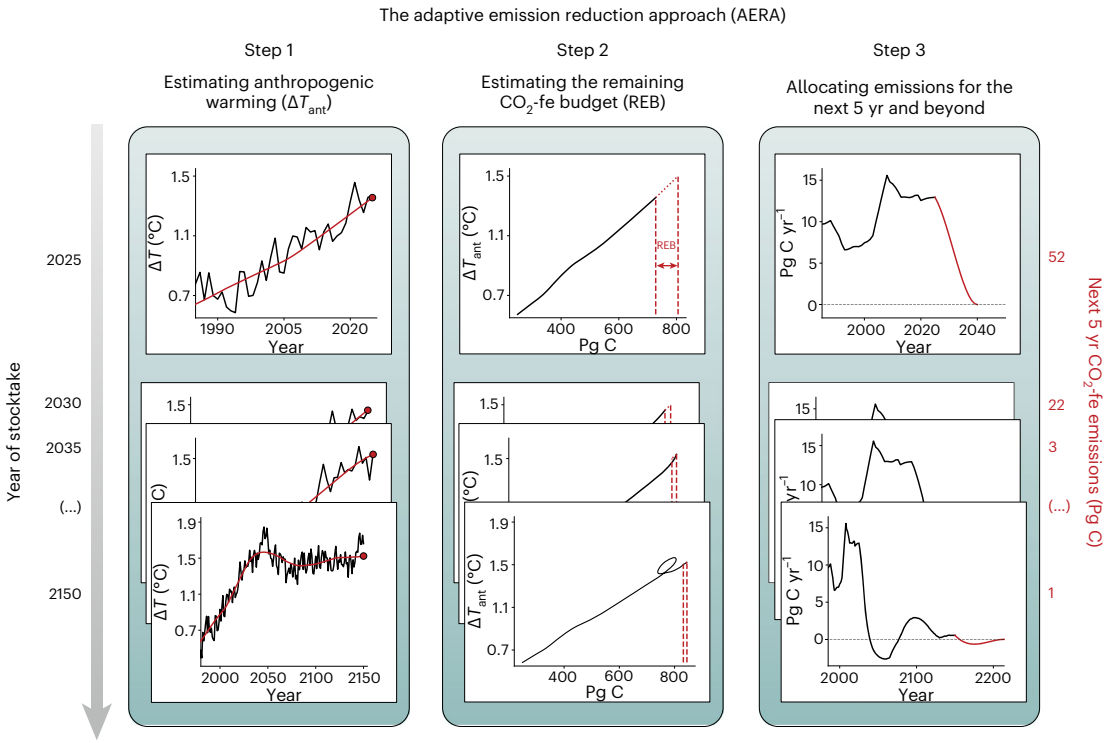

Fig. 1 | Schematic of the AERA to limit global warming. The three steps are repeated at the year of each stocktake (indicated on the left) to determine allowable emissions for the next 5 yr period (red numbers on the right) from temperature observations and forcing and emissions statistics. The approach is illustrated using results from one Bern3D-LPX simulation, with ECS = 3.2 °C as a surrogate for future observations (black lines in insets). Step 1. Estimation of the anthropogenic warming (red lines in inset) at the time of the stocktake from past time-series of GMST (black line) and anthropogenic radiative forcing. Step 2. Estimation of the remaining CO_2-fe emissions budget (REB; space between dashed red vertical lines) based on the observed linear relationship between anthropogenic warming (ΔT_{ant}) and cumulative CO_2-fe emissions (black line). Step 3. Allocation of the REB over the next 5 yr and beyond using a cubic function with minimal slope changes (red line). The approach stabilizes ΔT_{ant} close to the given target, here 1.5 °C, as illustrated in the bottom left inset.

precursors[8,22–25], historical CO_2-fe emissions[7], historical anthropogenic warming[26–29], change in temperatures after net-zero CO_2-fe emissions are reached[30], and future sources and sinks of CO_2 and other agents[30–36]. Furthermore, natural interannual-to-decadal variability in temperature[37–39], and land and ocean carbon and heat sinks[33,40] may mask the effects of GHG emissions reductions[41,42].

The large REB uncertainties may hamper efforts to establish ambitious NDCs and could potentially lead to insufficient global emissions reductions, large global warming, and severe consequences for natural and human systems[2,43,44]. Therefore, emissions reductions should be estimated at each stocktake using approaches that side-step these uncertainties and allow smoothly approaching a temperature target. Such approaches should be transparent, verifiable and, to the extent possible, objective to foster their acceptance as well as the implementation of the implied near-term emissions reduction measures. Such a science-based approach to guide near-term emissions reduction policies is currently missing.

The Adaptive Emission Reduction Approach

Here we propose the Adaptive Emission Reduction Approach (AERA) to estimate the necessary emissions reductions until temperature stabilization successively every 5 yr (for example, 2025, 2030, …) as foreseen by the stocktake mechanism. By adapting emissions every 5 yr, the AERA works like a control system that corrects emissions on the basis of realized warming to eventually approach a prescribed temperature target within a narrow range (±0.2 °C). For example, a temperature target of 1.75 °C may be chosen to estimate the emissions for keeping 'global warming well below 2 °C'. At a future stocktake, the temperature target can be redefined, for example 'to pursue efforts to limit it to 1.5 °C'.

The AERA only relies on global surface temperature observations, radiative forcing (RF) and emissions data, and does not rely on any Earth system model projections. Its adaptive nature ensures that emissions reductions that allow meeting the foreseen temperature target are quantified, irrespective of uncertainties in understanding the climate system. Such adaptive learning and stepwise adjustment of the emissions reduction target has been shown to help reduce costs[45] and avoid strong negative outcomes for the economy and the environment[44].

The AERA consists of three main steps: (1) determining the past anthropogenic warming and hence the remaining warming allowed, (2) estimating the remaining CO_2-fe emissions budget and (3) proposing a future CO_2-fe emissions curve until temperature stabilization (Fig. 1; see Methods). First, the anthropogenic warming is calculated from observed global mean surface temperature (GMST) time-series using the past RF of all relevant forcing agents (labelled as Step 1 in Fig. 1)[46]. This approach removes temperature changes from natural variability and non-anthropogenic forcing, such as volcanic eruptions and changes in solar activity, by fitting an impulse-response function (IRF)[47,48] to the RF and GMST time-series, leaving only the anthropogenic contribution to the observed warming. Alternatively, natural interannual-to-decadal variability in GMST may also be removed by applying a smoothing spline or another low-pass filter[49,50]. Once the realized anthropogenic warming is determined, the remaining warming between the temperature target and the realized anthropogenic warming is estimated by difference.

Second, the REB of CO_2-fe emissions is estimated using the transient climate response to cumulative emissions (TCRE)[51,52], determined as the ratio of past warming and past cumulative CO_2-fe emissions (Step 2 in Fig. 1). Mathematically, the REB is estimated as the remaining warming until the temperature target divided by the TCRE. Therefore,

we rely here on the near-linear relationship between cumulative CO_2-fe emission and past warming, and the assumption that this relationship holds for the near-future[14,53].

When quantified, the REB of CO_2-fe emissions is distributed over the future years (Step 3 in Fig. 1). Many possible future CO_2-fe emission curves may exist for one specific REB with different lengths and economic and political assumptions[54]. For simplicity, we use a cubic polynomial function and choose the parameters of the cubic function and its length, that is, the time until the REB is exhausted, by minimizing the curvature. Thereby, we assume that smaller changes in the trend of CO_2-fe emission curves are easier to implement. It may happen that the curve with the smallest curvature has positive emissions that are later compensated by negative emissions, which would result in a temporary temperature overshoot that could be harmful to the economy[55,56] and ecosystems[57,58]. To reduce the risk of such an overshoot, we also minimize exceedance emissions, that is, negative emissions if the REB is still positive or positive emissions if the REB is negative. A negative REB can occur if the anthropogenic warming or the TCRE turns out to be larger than estimated in previous stocktakes.

The three steps of the AERA are intended to be repeated every 5 yr at each stocktake (Fig. 1). At each stocktake, the determined future CO_2-fe emission curve until temperature stabilization can be split into contributions from CO_2, CH_4 and N_2O emissions, as well as contributions from other non-CO_2 forcing agents. This split may be achieved using a metric of choice, for example CO_2-fe emissions, which precisely capture the temperature change per CO_2-fe emission[7,15–17], or GWP-100[18,19,59], which is simpler but can nevertheless lead to relatively good results in terms of mitigation costs and climate outcomes[60,61]. Independent of the metric to split the CO_2-fe emissions into CO_2 and non-CO_2 emissions, the AERA adjusts the future CO_2-fe emissions curve every 5 yr on the basis of the most up-to-date observations of GMST, RF and CO_2-fe emissions. If the anthropogenic warming will turn out to be larger or smaller than anticipated by the time of the next stocktake, the adaptive nature of the AERA will adjust this successively, similar to a control system with a feedback loop. These regular adaptations successively correct for inherent uncertainties of the respective system, here the estimation of the realized anthropogenic warming and the response of GMST to anthropogenic emissions.

Testing the AERA with an Earth system model

Uncertainties are not explicitly considered in a control system, as in the AERA, but they determine how well the control system is functioning. We demonstrate that the AERA allows reaching a chosen temperature level, also those well below 2 °C, within the uncertainty with which the anthropogenic warming can be determined (±0.2 °C)[26–29], independent of uncertainties in the Earth's temperature sensitivity to GHGs and other agents, the strength of the land and ocean carbon sinks, radiative forcing estimates, the splitting of CO_2-fe emissions into CO_2, CH_4 and N_2O emissions and the applied method (CO_2-fe or GWP-100), and under deviations between emissions reductions quantified by the AERA versus those implemented. For this demonstration, we used the Earth system model of intermediate complexity, Bern3D-LPX[62,63], under nine different configurations with varying atmospheric sensitivity to atmospheric forcing agents and varying ocean mixing (see Methods). These configurations cover the range of estimates of the transient climate response (1.3–2.5 °C)[24] and equilibrium climate sensitivities (1.9–5.7 °C)[24] (see Methods). Depending on the configuration, the simulated anthropogenic warming in 2020 with prescribed historical CO_2 emissions and non-CO_2 radiative forcing ranges from 0.64 to 1.48 °C versus 1.23 ± 0.20 °C from observations (Extended Data Fig. 1). The remaining warming in the ensemble would deviate from the observational estimate when prescribing a fixed target in the model. To address the uncertainty in remaining emissions, the remaining warming in 2020 is set to the observational estimate (0.27 °C for the 1.5 °C target, see Methods) regardless of their simulated warming up to 2020.

Here we tested the AERA for two fixed temperature targets (1.5 °C and 2.0 °C) and for a peak and decline case with a temperature target of 1.75 °C until 2050 to 'keep global warming well below 2 °C'; however, from 2050 onwards, the target is reduced at each stocktake by 0.025 °C and reaches 1.5 °C in 2100 'to pursue efforts to limit it to 1.5 °C'[6]. The target could be further reduced to avoid any exceedance of the 1.5 °C limit. The choice of the extent to which CO_2-fe emissions are reduced by reducing CO_2 emissions versus reducing emissions of any other agents are not dictated by the AERA. We exemplify trade-offs in emissions by exploring different choices, for example, regarding GHG and aerosol emissions reductions. In the standard simulation, CO_2, CH_4 and N_2O emissions curves evolve proportionally in time after 2025 (Fig. 2d–f). An updated reduced form chemistry model[64] is used to calculate non-CO_2 GHG and aerosol radiative forcing from emissions (see Methods). Eventually, the emission curves for individual agents for which the resulting CO_2-fe emissions from all forcing agents best match the CO_2-fe emissions from the AERA are chosen. Atmospheric CO_2 and GMST for the next 5 yr period are then simulated by the Bern3D-LPX model using the AERA-estimated CO_2 fossil fuel emissions, non-CO_2 forcing and CO_2 emissions from land-use change. In the following paragraphs, CO_2 emissions refer only to the dynamically evolving fossil fuel emissions and not to the CO_2 emissions from prescribed land-use change.

The simulations demonstrate that the AERA allows reaching a chosen temperature level almost exactly at the end of the twenty-second century and already within the uncertainty to which anthropogenic warming can be determined (±0.2 °C)[26–29] in the second half of the twenty-first century, independent of the model's configuration (Fig. 2a). A temporal small overshoot may occur if the REB is initially overestimated.

For the fixed 1.5 °C target case, the resulting CO_2-fe emissions curves descend quickly (blue lines in Fig. 2b), reach zero CO_2-fe emissions by 2038 (2033–2048; the central estimate is the mean over 8 simulations with different superimposed interannual variability (see Methods) from the Equilibrium Climate Sensitivity (ECS) = 3.2 model configuration, and the range is the spread of the ensemble means across the remaining 8 model configurations with ECS varying from 1.9 °C to 5.7 °C), become negative afterwards, peak at −2.7 (−4.0 to −1.6) Pg C yr^{-1} and eventually converge to zero emissions after 2150. If CH_4 and N_2O emissions decrease strongly (Fig. 2e,f), net negative CO_2 emissions are not necessary to limit warming to 1.5 °C, but CO_2 emissions still approach zero emissions (Fig. 2d).

For the fixed 2.0 °C target, the resulting CO_2-fe emissions curves (orange lines in Fig. 2b) descend less rapidly than under the 1.5 °C target, reach zero emissions by 2070 (2050 to after 2300) and peak at negative emissions of −0.4 (−3.5 to +1.0) Pg C yr^{-1}. The cumulative CO_2 equivalent emissions for the 2 °C target, using GWP-100, are 310 Pg C until 2050 and 543 Pg C until 2100, as estimated from the AERA-derived CO_2, CH_4 and N_2O emissions. These CO_2 equivalent emissions are similar to estimates by the Climate Action Tracker[65] when assuming that all national pledges and targets are implemented (313 Pg C in 2050 and 513 Pg C in 2100), confirming that stabilizing warming at 2.0 °C is possible in this optimistic scenario[66]. Maximum annual CO_2-fe emissions reductions for the 2.0 °C target are considerably smaller than the necessary reductions for the 1.5 °C target (Fig. 2c). Furthermore, the timing when zero CO_2-fe emissions need to be reached are in line with previous estimates based on the time of the peak of radiative forcing[67].

The peak and decline case demonstrates that the AERA can also be applied with a temperature target that changes over time (green lines in Fig. 2). In the case where the temperature target is reduced from 1.75 °C in 2050 to 1.50 °C in 2100, the 2 °C warming is never exceeded. Negative CO_2-fe emissions are needed until the beginning of the twenty-second century. These negative CO_2-fe emissions are realized by negative CO_2 emissions because CH_4 and N_2O emissions have already reached their assumed minima due to the difficulty in

https://doi.org/10.1038/s41558-022-01537-9

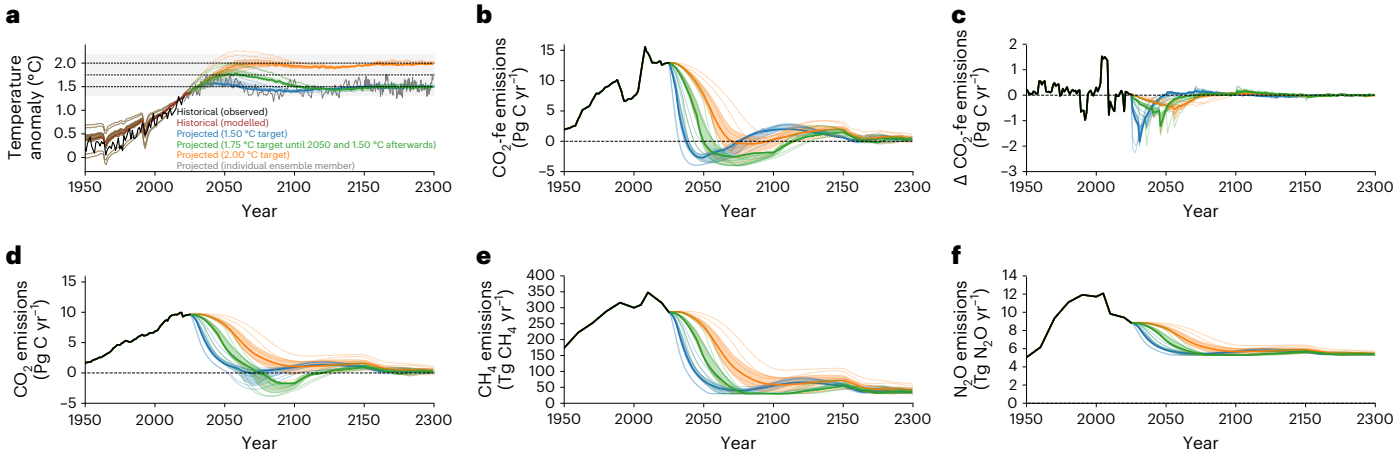

Fig. 2 | Globally averaged surface atmospheric temperature anomalies and GHG emissions following the AERA. a–c, Temperature anomalies with respect to 1850–1900 (**a**), CO_2-fe emissions (**b**) and their annual rate of change (**c**) if the AERA is applied every 5 yr starting in the year 2025 for the 1.5 °C target (blue) and the 2.0 °C target (orange). **d–f**, AERA-calculated emission curves for the proportionally evolving CO_2 (**d**), CH_4 (**e**) and N_2O (**f**). CO_2 emission curves shown here do not include emissions from prescribed land-use change. CH_4 and N_2O emissions cannot descend below the thresholds 30 Tg CH_4 yr^{-1} and 5.3 Tg N_2O yr^{-1} due to the difficulty in abating CH_4 and N_2O emissions from agricultural and livestock sectors (see Methods for the choice of these thresholds). Temperature and emission curves are also shown if the AERA is applied with a temperature target of 1.75 °C until 2050, and from 2050 onwards this target is reduced stepwise at each stocktake to 1.5 °C in 2100 (green). The thick solid lines show the average of the 8 simulations, with varying magnitude and timing of added interannual temperature variability of the Bern3D-LPX model configuration with an ECS of 3.2 °C. The thin solid lines show the same for the remaining 8 configurations covering ECS from 1.9 to 5.7 °C. The shaded area shows the range of all configurations that fall within the probable range of ECS as defined in ref. [24]. The grey shading in **a** indicates the uncertainty with which anthropogenic warming can be determined (±0.2 °C)[26–29] for the 1.5 °C and 2.0 °C targets.

abating CH_4 and N_2O emissions from agricultural and livestock sectors (see Methods). This peak and decline simulation shows that net-zero emissions in the second half of the twenty-first century (Article 4.1 of the Paris Agreement[6]) would be sufficient to 'keep global warming well below 2 °C', if strong emissions reductions were implemented in the first half of the twenty-first century.

The relative smoothness of the emission curves (Fig. 2b,d–f) demonstrates that the projected CO_2-fe emission curves as well as the associated CO_2, CH_4 and N_2O emissions curves by the AERA will need only relatively small adjustments every 5 yr. Therefore, the longer-term projections of CO_2-fe emission curves are reliable and less frequent adjustments may be sufficient. Even if CO_2-fe emission curves were adjusted by the AERA only every 10 yr, the resulting CO_2-fe emission curves look almost identical (Extended Data Fig. 2). However, small changes at every stocktake are still unavoidable as the REB remains uncertain. The initial REB guess can be different from the final emissions budget because the linearity between warming and cumulative emissions does not hold strictly in all configurations when emissions approach zero, partly due to unrealized warming (or cooling) from past CO_2-fe emission (that is, the zero-emission commitment[30]) that varies between model configurations. For Bern3D-LPX, temperatures decrease slightly in the decades after zero emissions are reached[30]. This decrease is automatically corrected by the AERA by slightly increasing CO_2-fe emissions. Despite these uncertainties in the initial estimate of the REB, the adaptive nature of the AERA allows reaching the temperature target while keeping changes in the CO_2-fe emission curve as small as possible.

Furthermore, we tested the robustness of the AERA under varying pathways of CH_4 and N_2O emission curves and aerosol radiative forcing, by performing three more simulations for the 1.5 °C target (Fig. 3; violet, red and ochre curves). Independent of the prescribed non-CO_2 emissions and radiative agents, the respective CO_2-fe emission curves remain almost indistinguishable and temperature stabilization is reached by the AERA in each case (Extended Data Fig. 3). However, the necessary CO_2 emissions reductions (Fig. 3a) depend strongly on the corresponding reduction in CH_4 and N_2O emissions and aerosol radiative forcing. When the magnitude of the aerosol forcing decreases faster (violet curves), slightly stronger reductions in CO_2, CH_4 and N_2O emissions are needed. In an idealized 'solar radiation management' case where aerosols are artificially emitted in the atmosphere after 2025 (red curves), CO_2, CH_4 and N_2O emissions reductions would only need to start 10–15 yr later than in the standard case (blue curves), while the necessary reduction rates of CO_2, CH_4 and N_2O emissions would remain similar. Moreover, once the solar radiation management would stop (not simulated here), strong reductions in CO_2, CH_4 and N_2O emissions would be immediately necessary[68,69]. In the extreme case where only emissions from non-CO_2 gases are reduced but CO_2 remains constant, temperature cannot be stabilized (Extended Data Fig. 4). Although reductions in non-CO_2 emissions can compensate for reductions in CO_2 emissions for some decades, continuing CO_2 emissions will lead to further increases in atmospheric CO_2 and hence in global temperature.

The almost identical temperature curves and associated CO_2-fe emission curves across these four scenarios with varying CH_4 and N_2O emissions as well as varying radiative forcing from aerosols (Extended Data Fig. 3) highlight the robustness of the CO_2-fe approach for transferring contributions from different radiative forcing agents to CO_2 equivalent emissions[7,15–17]. However, as the GWP-100 approach is widely used, for example, in the Paris Agreement, we tested the AERA using GWP-100 by repeating the standard simulations but using the GWP-100 and not the CO_2-fe metric to transfer CH_4 and N_2O emissions to CO_2 equivalent emissions (brown curves in Fig. 3). The AERA stabilizes the temperature at the given target when using GWP-100 (Extended Data Fig. 5). However, the limitations[7,15,17–19] of the GWP-100 metric lead to an initial overcorrection of the CO_2, CH_4 and N_2O emissions reductions by the AERA by up to 78% for CO_2 (maximum relative difference in emissions reductions since 2025) and 46% for CH_4 and N_2O that is later corrected by positive CO_2-fe emissions (brown curves in Fig. 3 and Extended Data Fig. 5b–f). However, when the usage of GWP is envisioned, better results may be achieved by using temperature change potentials[70] or adjustments to the GWP over time[61].

The behaviour of the AERA was further investigated assuming precautionary 'over-compliance' (using a REB that is smaller than the

https://doi.org/10.1038/s41558-022-01537-9

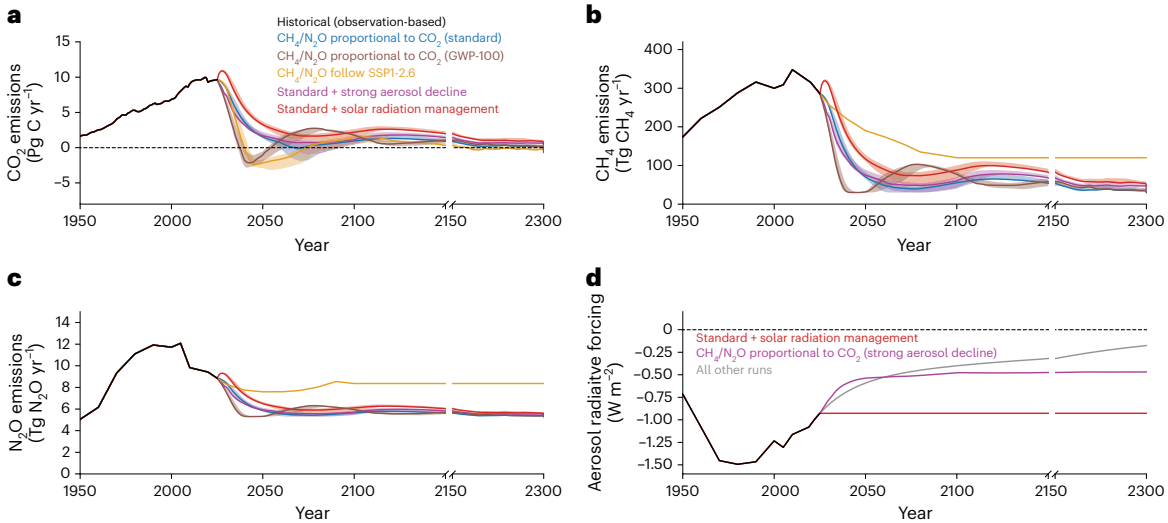

Fig. 3 | GHG emissions and aerosol radiative forcing following the AERA for the 1.5 °C temperature target using different assumptions for non-CO_2 radiative forcing agents. a–d, Emissions of CO_2 (**a**), CH_4 (**b**) and N_2O (**c**), and the total radiative forcing of anthropogenic aerosols (stratospheric and tropospheric) (**d**) for five different idealized cases: aerosol radiative forcing decreases exponentially and CO_2, CH_4 and N_2O emissions evolve proportionally (blue, identical to blue lines in Fig. 1); aerosol radiative forcing decreases exponentially and CO_2, CH_4 and N_2O emissions evolve proportionally but GWP-100 is used to split CO_2 equivalent emissions instead of the CO_2-fe approach (brown); aerosol radiative forcing decreases more strongly due to strong CO_2 emissions cuts[72,73] and CO_2, CH_4 and N_2O emissions evolve proportionally (violet); aerosol radiative forcing decreases exponentially but CH_4 and N_2O emissions follow SSP1-2.6 after 2025 and only CO_2 evolves dynamically (ochre); and aerosol radiative forcing remains constant after 2025 and CO_2, CH_4 and N_2O emissions evolve proportionally (red, idealized solar radiation management). CO_2 emission curves shown here do not include emissions from prescribed land-use change. The thick solid lines show the average of the 8 simulations, with varying magnitude and timing of added interannual temperature variability of the Bern3D-LPX model configuration with an ECS of 3.2 °C. The shaded area shows the range of all configurations that fall within the probable range of ECS as defined in ref. [24]. The corresponding temperature curves, CO_2-fe emissions and CO_2 equivalent emissions for each simulated case are shown in Extended Data Fig. 3 (all except GWP-100 case) and Extended Data Fig. 5 (GWP-100 case).

central estimate, that is, 67th and 83rd percentiles instead of the 50th percentile) or 'under-compliance' (using a REB that is higher than the central estimate, that is, 17th and 33rd percentiles). In the case of 'under-compliance', the target temperature is still reached but at the cost of a larger temperature overshoot (Extended Data Figs. 6 and 7). In the case of 'over-compliance', the temperature target is also reached, and the temperature overshoot can be avoided or reduced (for the highest ECS). Overall, the AERA thus provides a robust and working tool to estimate the necessary emissions reductions to minimize the risk of temperature overshoot and the risk of surpassing a given temperature limit (for example, of 2 °C).

Applying the AERA in 2020

Having demonstrated the robustness and fidelity of the AERA in the model world, the question arises as to what rate of emissions reductions the AERA would have estimated for the 1.5 °C and 2.0 °C temperature targets on the basis of available observations and emissions statistics in 2020, when 186 parties had communicated their first NDCs to the United Nations Framework Convention on Climate Change (UNFCCC) Secretariat. Applied to observational data until 2020, step one of the AERA yields an anthropogenic warming of 1.23 °C, resulting in a remaining warming of 0.27 °C for the 1.5 °C target and 0.77 °C for the 2.0 °C target. In step 2, the ratio of the anthropogenic warming of 1.23 °C and past cumulative CO_2-fe emissions of 749 Pg C results in an REB of 167 Pg C for 1.5 °C and 472 Pg C for 2.0 °C. These remaining CO_2-fe emissions are divided over the coming years in step 3 of the AERA, assuming a cubic polynomial function with minimum changes to its slope. The so-estimated reduction in annual CO_2-fe emissions from 2020 to 2025 is 3.7 Pg C for the 1.5 °C temperature target (from 13.7 Pg C yr^{-1} in 2020 to 10.0 Pg C yr^{-1} in 2025) and 1.0 Pg C for the 2.0 °C temperature target (from 13.7 Pg C yr^{-1} in 2020 to 12.6 Pg C yr^{-1} in 2025). Beyond 2025, CO_2-fe emissions would have to drop to 7.0 Pg C yr^{-1} in 2030 to reach the 1.5 °C target, further decrease to 0.5 Pg C yr^{-1} in 2050 and become lightly negative after 2055 (up to −0.5 Pg C yr^{-1}) until reaching zero CO_2-fe emissions in 2085. For the 2.0 °C target, CO_2-fe emissions would have to reach 11.3 Pg C yr^{-1} in 2030, 7.2 Pg C yr^{-1} in 2050 and zero CO_2-fe emissions by 2110. While the estimates of past warming, TCRE, REB and necessary emissions reductions have uncertainties, the AERA side-steps these uncertainties. The successive adaptation of the CO_2-fe emissions every 5 yr allows correction of the emission pathway over time if the initial estimates were not exact. Estimates are based on the median (50th percentile) value in these example calculations for year 2020. Other percentiles may be used, as in the 'over-compliance case' described previously, for considering the precautionary principle of the UNFCCC.

Discussion

The AERA estimates future CO_2-fe emission pathways that allow reaching a desired temperature target within the uncertainty to which anthropogenic warming can be determined (±0.2 °C)[26–29]. Climate projections by Earth system models using the AERA can be incorporated into the periodical IPCC Assessment Reports and provide an alternative to the often-used approach of applying predefined emissions or concentration pathways (such as Shared Socioeconomic Pathways (SSPs)). Such pathways are generally designed a priori to be consistent with a given radiative forcing or warming level (for example, SSP1-1.9 for 1.9 W m^{-2} and 1.5 °C by 2100), without knowing the actual response of the Earth system to these emissions pathways[71]. AERA-based warming simulations from different models would be directly comparable in terms of impacts under equal warming. However, the sociotechnical feasibility of the pathways is not informed by the AERA but could be assessed by coupling these simulations to a cost-effectiveness integrative assessment model in a recursive dynamic setup. The approach may thus guide a valuable and highly policy-relevant complementary set of

simulations for the next phase of the Coupled Model Intercomparison Project to result in a range of emission curves that all produce the same warming in the long-term as opposed to current simulations with the same emission or concentration curves that can result in very different levels of warming.

In the Paris Agreement, the 2 °C warming limit represents an upper threshold that should not be passed. The AERA applied with the median observation-based estimates allows to devise pathways that keep warming to within about 0.2 °C of prescribed warming targets. To keep warming below upper temperature limits that have been set for global warming allowable to society, the AERA can be applied with a temperature target about 0.2 °C lower than such limits or by using a lower-than-the-median estimate for the REB as in the 'over-compliance case'. In future efforts, the approach could be further refined by applying the AERA within a fully observation-constrained probabilistic framework[12,13] to estimate the necessary emissions reductions with associated likelihoods.

The AERA presents policymakers with transparent science- and observation-based emissions reductions that would be necessary to limit global warming to any chosen temperature level without the need to make climate projections with Earth system models. With many simulations, substituting for future real-world outcomes, we have shown that this approach is robust across a vast number of possible developments. Policymakers may wish to use the information from the AERA to regularly update near- and long-term emission reduction goals, including additional socio-economic considerations such as equity, mitigation versus adaptation costs, and risks of not meeting a target. The AERA can thereby help to successfully 'keep global warming well below 2 °C and pursue efforts to limit it to 1.5 °C'[6].

Online content

Any methods, additional references, Nature Portfolio reporting summaries, source data, extended data, supplementary information, acknowledgements, peer review information; details of author contributions and competing interests; and statements of data and code availability are available at https://doi.org/10.1038/s41558-022-01537-9.

References

1. *State of the Global Climate 2020* (World Meteorological Organization, 2021).
2. Allen, M. R. et al. in *Special Report on Global Warming of 1.5 °C* (eds Masson-Delmotte, V. et al.) Ch. 1 (WMO, 2018).
3. *Special Report on the Ocean and Cryosphere in a Changing Climate* (IPCC, 2019).
4. Hoegh-Guldberg, O. et al. The human imperative of stabilizing global climate change at 1.5 °C. *Science* **365**, eaaw6974 (2019).
5. Hoegh-Guldberg, O. et al. in *Special Report on Global warming of 1.5 °C* (eds Masson-Delmotte, V. et al.) Ch. 3 (WMO, 2018).
6. *Paris Agreement. Report of the Conference of the Parties to the United Nations Framework Convention on Climate Change* (UNFCCC, 2015).
7. Jenkins, S., Millar, R. J., Leach, N. & Allen, M. R. Framing climate goals in terms of cumulative CO_2-forcing-equivalent emissions. *Geophys. Res. Lett.* **45**, 2795–2804 (2018).
8. Rogelj, J., Forster, P. M., Kriegler, E., Smith, C. J. & Séférian, R. Estimating and tracking the remaining carbon budget for stringent climate targets. *Nature* **571**, 335–342 (2019).
9. Matthews, H. D. et al. Opportunities and challenges in using remaining carbon budgets to guide climate policy. *Nat. Geosci.* **13**, 769–779 (2020).
10. Tokarska, K. B. & Gillett, N. P. Cumulative carbon emissions budgets consistent with 1.5 °C global warming. *Nat. Clim. Change* **8**, 296–299 (2018).
11. Peters, G. P. Beyond carbon budgets. *Nat. Geosci.* **11**, 378–380 (2018).
12. Damon Matthews, H. et al. An integrated approach to quantifying uncertainties in the remaining carbon budget. *Commun. Earth Environ.* **2**, 7 (2021).
13. Steinacher, M., Joos, F. & Stocker, T. F. Allowable carbon emissions lowered by multiple climate targets. *Nature* **499**, 197–201 (2013).
14. IPCC. in *Climate Change 2013: The Physical Science Basis* (eds Stocker, T. F. et al.) 1–30 (Cambridge Univ. Press, 2013).
15. Allen, M. R. et al. A solution to the misrepresentations of CO_2-equivalent emissions of short-lived climate pollutants under ambitious mitigation. *npj Clim. Atmos. Sci.* **1**, 16 (2018).
16. Wigley, T. M. L. The Kyoto Protocol: CO_2 CH_4 and climate implications. *Geophys. Res. Lett.* **25**, 2285–2288 (1998).
17. Smith, M. A., Cain, M. & Allen, M. R. Further improvement of warming-equivalent emissions calculation. *npj Clim. Atmos. Sci.* **4**, 19 (2021).
18. Tanaka, K. & O'Neill, B. C. The Paris Agreement zero-emissions goal is not always consistent with the 1.5 °C and 2 °C temperature targets. *Nat. Clim. Change* **8**, 319–324 (2018).
19. Allen, M. et al. Ensuring that offsets and other internationally transferred mitigation outcomes contribute effectively to limiting global warming. *Environ. Res. Lett.* **16**, 74009 (2021).
20. *Report of the Conference of the Parties serving as the meeting of the Parties to the Paris Agreement on the third part of its first session, held in Katowice from 2 to 15 December 2018. Addendum 2. Part two: Action taken by the Conference of the Parties serving as the meeting of the Parties to the Paris Agreement* FCCC/PA/CMA/2018/3/Add.2, 18/CMA.1, para 37 (UNFCC, 2019).
21. Arias, P. A. et al. Technical Summary. in *Climate Change 2021: The Physical Science Basis* (eds Masson-Delmotte, V. et al.) 33–144 (Cambridge Univ. Press, 2021).
22. Meehl, G. A. et al. Context for interpreting equilibrium climate sensitivity and transient climate response from the CMIP6 Earth system models. *Sci. Adv.* **6**, eaba1981 (2022).
23. Nijsse, F. J. M. M., Cox, P. M. & Williamson, M. S. Emergent constraints on transient climate response (TCR) and equilibrium climate sensitivity (ECS) from historical warming in CMIP5 and CMIP6 models. *Earth Syst. Dyn.* **11**, 737–750 (2020).
24. Sherwood, S. C. et al. An assessment of Earth's climate sensitivity using multiple lines of evidence. *Rev. Geophys.* **58**, e2019RG000678 (2020).
25. Tokarska, K. B. et al. Past warming trend constrains future warming in CMIP6 models. *Sci. Adv.* **6**, eaaz9549 (2021).
26. Haustein, K. et al. A real-time Global Warming Index. *Sci. Rep.* **7**, 15417 (2017).
27. Ribes, A., Qasmi, S. & Gillett, N. P. Making climate projections conditional on historical observations. *Sci. Adv.* **7**, eabc0671 (2022).
28. Gillett, N. P. et al. Constraining human contributions to observed warming since the pre-industrial period. *Nat. Clim. Change* **11**, 207–212 (2021).
29. IPCC. in *Climate Change 2021: The Physical Science Basis* (eds Masson-Delmotte, V. et al.) 3–32 (Cambridge Univ. Press, 2021).
30. MacDougall, A. H. et al. Is there warming in the pipeline? A multi-model analysis of the Zero Emissions Commitment from CO_2. *Biogeosciences* **17**, 2987–3016 (2020).
31. Saunois, M. et al. The global methane budget 2000–2017. *Earth Syst. Sci. Data* **12**, 1561–1623 (2020).
32. Heinze, C. et al. ESD reviews: climate feedbacks in the Earth system and prospects for their evaluation. *Earth Syst. Dyn.* **10**, 379–452 (2019).
33. Friedlingstein, P. et al. Global carbon budget 2020. *Earth Syst. Sci. Data* **12**, 3269–3340 (2020).
34. Arora, V. K. et al. Carbon–concentration and carbon–climate feedbacks in CMIP6 models and their comparison to CMIP5 models. *Biogeosciences* **17**, 4173–4222 (2020).

35. Jones, C. D. & Friedlingstein, P. Quantifying process-level uncertainty contributions to TCRE and carbon budgets for meeting Paris Agreement climate targets. *Environ. Res. Lett.* **15**, 074019 (2020).
36. Tian, H. et al. A comprehensive quantification of global nitrous oxide sources and sinks. *Nature* **586**, 248–256 (2020).
37. Thompson, D. W. J., Wallace, J. M., Jones, P. D. & Kennedy, J. J. Identifying signatures of natural climate variability in time series of global-mean surface temperature: methodology and insights. *J. Clim.* **22**, 6120–6141 (2009).
38. Medhaug, I., Stolpe, M. B., Fischer, E. M. & Knutti, R. Reconciling controversies about the 'global warming hiatus'. *Nature* **545**, 41–47 (2017).
39. Turner, J. et al. Absence of 21st century warming on Antarctic Peninsula consistent with natural variability. *Nature* **535**, 411–415 (2016).
40. Watanabe, M. et al. Strengthening of ocean heat uptake efficiency associated with the recent climate hiatus. *Geophys. Res. Lett.* **40**, 3175–3179 (2013).
41. Peters, G. P. et al. Towards real-time verification of CO_2 emissions. *Nat. Clim. Change* **7**, 848–850 (2017).
42. Spring, A., Ilyina, T. & Marotzke, J. Inherent uncertainty disguises attribution of reduced atmospheric CO_2 growth to CO_2 emission reductions for up to a decade. *Environ. Res. Lett.* **15**, 114058 (2020).
43. Steffen, W. et al. Trajectories of the earth system in the anthropocene. *Proc. Natl Acad. Sci. USA* **115**, 8252 (2018).
44. Oppenheimer, M., O'Neill, B. C. & Webster, M. Negative learning. *Clim. Change* **89**, 155–172 (2008).
45. Webster, M., Jakobovits, L. & Norton, J. Learning about climate change and implications for near-term policy. *Clim. Change* **89**, 67–85 (2008).
46. Otto, F. E. L., Frame, D. J., Otto, A. & Allen, M. R. Embracing uncertainty in climate change policy. *Nat. Clim. Change* **5**, 917–920 (2015).
47. Held, I. M. et al. Probing the fast and slow components of global warming by returning abruptly to preindustrial forcing. *J. Clim.* **23**, 2418–2427 (2010).
48. Joos, F. et al. Carbon dioxide and climate impulse response functions for the computation of greenhouse gas metrics: a multi-model analysis. *Atmos. Chem. Phys.* **13**, 2793–2825 (2013).
49. Enting, I. G. On the use of smoothing splines to filter CO_2 data. *J. Geophys. Res. Atmos.* **92**, 10977–10984 (1987).
50. Luo, J., Ying, K. & Bai, J. Savitzky–Golay smoothing and differentiation filter for even number data. *Signal Process.* **85**, 1429–1434 (2005).
51. Allen, M. R. et al. Warming caused by cumulative carbon emissions towards the trillionth tonne. *Nature* **458**, 1163–1166 (2009).
52. Matthews, H. D., Gillett, N. P., Stott, P. A. & Zickfeld, K. The proportionality of global warming to cumulative carbon emissions. *Nature* **459**, 829–832 (2009).
53. IPCC. in *Climate Change 2014: Synthesis Report* (eds Pachauri, R. K. & Meyer, L. A.) 1–32 (IPCC, 2014).
54. Edwards, M. R., McNerney, J. & Trancik, J. E. Testing emissions equivalency metrics against climate policy goals. *Environ. Sci. Policy* **66**, 191–198 (2016).
55. Ricke, K. L., Millar, R. J. & MacMartin, D. G. Constraints on global temperature target overshoot. *Sci. Rep.* **7**, 14743 (2017).
56. Parry, M., Lowe, J. & Hanson, C. Overshoot, adapt and recover. *Nature* **458**, 1102–1103 (2009).
57. Anderson, C. M. et al. Planning for change: conservation-related impacts of climate overshoot. *Bioscience* **70**, 115–118 (2020).
58. de Vrese, P. & Brovkin, V. Timescales of the permafrost carbon cycle and legacy effects of temperature overshoot scenarios. *Nat. Commun.* **12**, 2688 (2021).
59. Myhre, G. et al. in *Climate Change 2013: The Physical Science Basis* (eds Stocker, T. F. et al.) Ch. 8 (Cambridge Univ. Press, 2013).
60. Harmsen, M. J. H. M. et al. How climate metrics affect global mitigation strategies and costs: a multi-model study. *Clim. Change* **136**, 203–216 (2016).
61. Tanaka, K., Boucher, O., Ciais, P., Johansson, D. J. A. & Morfeldt, J. Cost-effective implementation of the Paris Agreement using flexible greenhouse gas metrics. *Sci. Adv.* **7**, eabf9020 (2022).
62. Roth, R., Ritz, S. P. & Joos, F. Burial-nutrient feedbacks amplify the sensitivity of atmospheric carbon dioxide to changes in organic matter remineralisation. *Earth Syst. Dyn.* **5**, 321–343 (2014).
63. Lienert, S. & Joos, F. A Bayesian ensemble data assimilation to constrain model parameters and land-use carbon emissions. *Biogeosciences* **15**, 2909–2930 (2018).
64. Joos, F. et al. Global warming feedbacks on terrestrial carbon uptake under the Intergovernmental Panel on Climate Change (IPCC) Emission Scenarios. *Glob. Biogeochem. Cycles* **15**, 891–907 (2001).
65. *Climate Action Tracker* (Climate Analytics and NewClimate Institute, accessed December 2021); https://climateactiontracker.org/global/temperatures/
66. Meinshausen, M. et al. Realization of Paris Agreement pledges may limit warming just below 2 °C. *Nature* **604**, 304–309 (2022).
67. Wigley, T. M. L. The relationship between net GHG emissions and radiative forcing with an application to Article 4.1 of the Paris Agreement. *Clim. Change* **169**, 13 (2021).
68. Wigley, T. M. L. A combined mitigation/geoengineering approach to climate stabilization. *Science* **314**, 452–454 (2006).
69. Robock, A., Oman, L. & Stenchikov, G. L. Regional climate responses to geoengineering with tropical and Arctic SO_2 injections. *J. Geophys. Res. Atmos.* **113**, D16101 (2008).
70. Shine, K. P., Berntsen, T. K., Fuglestvedt, J. S., Skeie, R. B. & Stuber, N. Comparing the climate effect of emissions of short- and long-lived climate agents. *Phil. Trans. R. Soc. A* **365**, 1903–1914 (2007).
71. O'Neill, B. C. et al. The Scenario Model Intercomparison Project (ScenarioMIP) for CMIP6. *Geosci. Model Dev.* **9**, 3461–3482 (2016).
72. Rogelj, J. et al. Air-pollution emission ranges consistent with the representative concentration pathways. *Nat. Clim. Change* **4**, 446–450 (2014).
73. Lamboll, R. D., Nicholls, Z. R. J., Kikstra, J. S., Meinshausen, M. & Rogelj, J. Silicone v1.0.0: an open-source Python package for inferring missing emissions data for climate change research. *Geosci. Model Dev.* **13**, 5259–5275 (2020).

Methods

AERA

The AERA[74] is designed to estimate a future trajectory of CO_2 forcing equivalent (CO_2-fe) emissions to reach a temperature target. The AERA is formulated as part of a control system with a feedback loop. In a control system, the output of a system is controlled by regularly adjusting the input to the system on the basis of the deviation between the actual and target value of a process variable. An example is the regulation of room temperature with a heating-cooling unit. The room temperature is measured to estimate the deviation between the actual and target temperature. The flow of heat between the unit and the room is then adjusted by the 'controller' on the basis of the deviation and the median available estimate of the response of room temperature to heat flow. This procedure is repeated, for example, every minute, to adjust the room temperature towards and to track the target temperature. Similarly, the AERA, when implemented with real-world emissions, will control the evolution of anthropogenic warming by adjusting CO_2-fe emissions. Here, emissions are foreseen to be adjusted every 5 yr on the basis of the median observational estimate of the deviation between actual and target anthropogenic warming and the median observation-based estimate of the Earth system's response to emissions. Implementing the regularly updated emissions reductions following the AERA will allow the temperature to converge towards the target temperature, despite uncertainties in our understanding of the Earth System.

As input, the AERA requires past global time-series of three variables: (1) global mean surface temperature (GMST), (2) total anthropogenic radiative forcing (RF) and (3) total CO_2-fe emissions from CO_2, non-CO_2 GHGs, precursors, aerosols and land-use change combined (see CO_2-fe emissions calculation below). The AERA contains three steps. First, internal variability from the GMST record is removed by calculating anthropogenic warming from the GMST time-series[46]. Second, the REB[2,7–9] is estimated on the basis of the near-linear relationship between past CO_2-fe emissions and warming (that is, the transient climate response to cumulative carbon emission)[51,52], and the remaining temperature gap before the target temperature will be reached. Third, this REB is distributed over the future years using a cubic polynomial function. The three steps are to be repeated every 5 yr. Therefore, the future CO_2-fe emission curve may be adjusted every 5 yr on the basis of the most up-to-date observations of GMST, RF and CO_2-fe emissions.

In the first step, the natural internal and external (that is, volcanoes, solar activity) variability is removed from the observed historical GMST, resulting in a temperature curve (T_{ant}) that only changes due to anthropogenic forcing. T_{ant} is determined following ref. [46] by fitting an IRF[47,48] to the observed GMST(t). The IRF features three characteristic timescales, τ_i, and coefficients, a_i:

$$T_{ant}(t) = T_{ant}(1850) + c\int_{1850}^{t} I_{RF}(t') \left(a_1\left(1-e^{\frac{-(t-t')}{\tau_1}}\right) + a_2\left(1-e^{\frac{-(t-t')}{\tau_2}}\right) + a_3\left(1-e^{\frac{-(t-t')}{\tau_3}}\right)\right)dt'. \quad (1)$$

Equation (1) relates the sum of step-like changes in RF (impulses $I_{RF}(t')$, defined as the change in RF in year t') over the past observed period to $T_{ant}(t)$. The constant c is a scaling and unit conversion factor, and the integral is approximated by the sum of annual values. The seven free parameters of equation (1) (timescales τ_1, τ_2 and τ_3; coefficients a_1, a_2; c; T_{ant} (1850)) are determined to best fit the observation-based GMST by minimizing the root-mean-square deviations between $T_{ant}(t)$ and GMST(t). The parameters are determined at each stocktake to account for possible feedbacks from the warming of the climate and cumulative CO_2 uptake that may change the shape of the IRF[75]. The free parameters were constrained a priori to ease the fitting. The timescales are limited to 1.5–2.0 yr (for τ_1), 15–30 yr (τ_2) and 100–600 yr (τ_3), and the coefficients are limited to 0.2–0.4 (a_1) and 0.3–0.5 (a_2). a_3 is calculated by $a_3 = 1 - a_1 - a_2$. Implicitly, a_3 is thus limited to 0.1–0.5. These broad constraints are enforced to ensure physically meaningful parameters. From the anthropogenic temperature time-series $T_{ant}(t)$, the anthropogenic temperature anomaly (ΔT_{ant}) is calculated by subtracting the mean GMST(t) over the reference period 1850–1900 from T_{ant}:

$$\Delta T_{ant}(t) = T_{ant}(t) - \overline{\mathrm{GMST}(1850-1900)}. \quad (2)$$

The REB of CO_2-fe emissions is estimated at the time of the stocktake, t_{st} (years 2025, 2030, ...), exploiting the near-linearity between warming and cumulative CO_2 emissions[14,53]. The REB (t_{st}) is determined by multiplying the remaining anthropogenic temperature anomaly until the target temperature is reached with the ratio of cumulative CO_2-fe emissions since 1850 $\left(\int_{1850}^{t_{st}} E_{fe}^{CO_2}(t')\,dt'\right)$ and the realized anthropogenic warming anomaly $\Delta T_{ant}(t_{st})$[51,52]:

$$\mathrm{REB}(t_{st}) = \left(\Delta T_{ant}^{target} - \Delta T_{ant}(t_{st})\right)\frac{\int_{1850}^{t_{st}} E_{fe}^{CO_2}(t')\,dt'}{\Delta T_{ant}(t_{st})}, \quad (3)$$

with ΔT_{ant}^{target} being the temperature target, for example, 1.5 °C or 2 °C.

The emission pathway for the 5 yr following the stocktake is determined by distributing the remaining CO_2-fe emission budget over the future years using a cubic polynomial function:

$$E_{fe}^{CO_2}(t) = at^3 + bt^2 + ct + d \quad \text{for } t_{target} \geq t \geq t_{st}, \quad (4)$$

with t referring to the time after the year of the stocktake (t_{st}) and t_{target} being the year when the temperature target should be reached. The t_{target} is not an a priori fixed year[61,70] but continuous, to evolve over time and is adapted here to ensure that the change in the slope of CO_2-fe emissions remains as small as possible (see paragraph below). The parameters a, b, c and d are chosen to determine an emission curve with a small curvature using the following boundary conditions:

(1) $E_{fe}^{CO_2}(t_{st})$ equals the CO_2-fe emissions at the year of the stocktake.
(2) Changes in $E_{fe}^{CO_2}$ in the year before the stocktake are as close as possible to changes in $E_{fe}^{CO_2}$ at the year of the stocktake:

$$\frac{\partial E_{fe}^{CO_2}}{\partial t}(t_{st}) = \frac{\partial E_{fe}^{CO_2}}{\partial t}(t_{st}-1) + \eta, \quad (5)$$

with η being a change in the slope.
(3) $E_{fe}^{CO_2}(t_{target})$ equals zero.
(4) $E_{fe}^{CO_2}$ remains constant after the target year is reached ($\frac{\partial E_{fe}^{CO_2}}{\partial t}(t_{target}) = 0$)

Condition (1) enforces the polynomial function to match emissions at the time of the stocktake. Condition (2) minimizes the changes in the emissions trend around the stocktake, thereby implicitly accounting for inertia in the socio-economic system that makes it difficult to 'abruptly' change trends. Conditions (3) and (4) imply that CO_2-fe emissions are zero when the target is reached and stay zero afterwards in the absence of any trend change in emissions. These boundary conditions leave two free parameters t_{target} and η. For each combination of these two parameters, one emission curve exists. The maximum length of the time-series (t_{max}) varies dynamically depending on the REB and the CO_2-fe emissions in the year of the stocktake:

$$t_{max} = 30\mathrm{yr} + 90\mathrm{yr} \times e^{\left(-\frac{|\max(\mathrm{REB}-30\,\mathrm{Pg\,C},\,0\,\mathrm{Pg\,C})|}{50\,\mathrm{Pg\,C}}\right)} + \min\left(\left|E_{fe}^{*CO_2}(t_{st})\right|, 10\,\frac{\mathrm{Pg\,C}}{\mathrm{yr}}\right)^2 \times \frac{\mathrm{yr}^3}{(\mathrm{Pg\,C})^2}. \quad (6)$$

Each term in equation (6) is rounded to its nearest integer. This dynamic definition keeps the time until when the temperature target should be reached (t_{max}) relatively short (close to 30 yr, first term in

equation (6)) so that the temperature does not remain off target for too long. However, in two cases, it is preferable for the REB to be distributed over a longer time. The first case occurs when the anthropogenic warming is close to the temperature target. In that case, a short t_{max} leads to abrupt short-term changes in CO_2-fe emissions because a small REB (<-100 Pg C) is forced into a small number of years (Supplementary Fig. 1). To avoid such an oscillation, t_{max} increases by up to an additional 90 yr when the REB becomes small (term 2 in equation (6)). The second case occurs when the REB is large but annual emissions are still high (>~5 Pg C yr^{-1}). These high emissions will already be correcting the temperatures over time. A reduced t_{max} would force the large REB into a small number of years and cause even higher emissions in the first years, which need to be reduced shortly afterwards (Supplementary Fig. 1). The third term in equation (6), with $E_{fe}^{*CO_2}(t_{st})$ being equal to $E_{fe}^{CO_2}(t_{st})$ if the REB and $E_{fe}^{CO_2}(t_{st})$ have the same sign and being zero otherwise, increases t_{max} by up to 100 yr. Overall, the choice of the different timescales does not rely on theoretical assumptions, but it is a result of tests across a wide range of timescales.

For determining the free parameters t_{target} and η, we systematically varied them in steps of 1 yr and 0.1 Pg C yr^{-2} within the following limits: 5 yr < $(t_{target} - t_{st}) < t_{max}$; -2.5 Pg C $yr^{-2} < \eta < 2.5$ Pg C yr^{-2}. The 'best' choice out of these emission curves is chosen in three steps:

First, all curves whose integrated emissions from t_{st} to t_{target} do not agree with the REB within ±5 Pg C ($|\xi| < 5$ Pg C) are excluded:

$$\xi = \int_{t_{st}}^{t_{target}} E_{fe}^{CO_2}(t')\,dt' - \mathrm{REB}, \tag{7}$$

with ξ being the difference between the REB and the integral of the CO_2-fe emission curve. In our tests, at every stocktake, at least one CO_2-fe emissions curve with a REB that lies within ±5 Pg C of the REB determined by the AERA is found. In the potential cases where a curve within the REB limit cannot be found, the curve with the smallest $|\xi|$ would be chosen.

Second, among the remaining curves, all curves with exceedance emissions (ε) larger than 10 Pg C are excluded. Exceedance emissions are defined as follows:

$$\int_{t_{st}}^{t_{target}} \left|E_{fe}^{CO_2}(t')\right| dt' - \int_{t_{st}}^{t_{target}} E_{fe}^{CO_2}(t')\,dt' < 2\varepsilon. \tag{8}$$

The left side of equation (8) describes the difference between the integral of the absolute emissions over time and the emissions integral. Although this difference is ideally zero, it can diverge if $E_{fe}^{CO_2}(t')$ changes its sign between t_{st} and t_{target}. This can, for example, be the case if $E_{fe}^{CO_2}(t_{st})$ is still positive and $T_{ant}(t_{st})$ is already larger than the temperature target. Thus, the still emitted positive emissions before emissions become negative increase the exceedance of T_{ant} further and are therefore called 'exceedance emissions'. They are later compensated by the roughly similar amount of negative emissions, hence the factor 2 on the right side of equation (8). Several studies[76–79] have shown that the global warming response to positive and negative CO_2 emissions is indeed approximately symmetrical for moderate amounts of negative emissions and under ambitious climate targets.

In 99.95% of the cases, a CO_2-fe emissions curve with exceedance emissions smaller than 10 Pg C is found. In the remaining 0.05% of cases, the curve with the smallest exceedance emissions is chosen. In the 99.95% of the cases where the limits for $|\xi|$ and exceedance emissions are met, the curve with the combination of t_{target} and η that results in the smallest curvature (sum of absolute changes in emissions change) is retained. The smallest curvature is calculated by minimizing the sum of each curve's (absolute) second derivates from year $t_{st} - 1$ to year t_{target}.

CO_2-fe emissions from non-CO_2 agents

The historical CO_2-fe emissions from non-CO_2 agents are estimated on the basis of the radiative forcing time-series of non-CO_2 agents. This annual time-series is translated into CO_2-fe emissions[17]:

$$\alpha E_{CO_2-fe}(t) = \frac{dF_{non-CO_2}(t)}{dt} + \rho F_{non-CO_2}(t), \tag{9}$$

with $F_{non-CO_2}(t)$ being the radiative forcing of non-CO_2 agents, $E_{CO_2-fe}(t)$ being CO_2-fe emissions from non-CO_2 agents, ρ being the rate of decline in radiative forcing over these timescales under zero emissions (0.33%), and α being a constant representing the forcing impact of ongoing CO_2 emissions (1.08 W m^{-2} per 1,000 $GtCO_2$).

Applying the AERA to observations until 2020

The necessary emissions reductions in 2020 are quantified using the AERA. As input, we used the historical GMST data from HadCRUT5 (https://crudata.uea.ac.uk/cru/data/temperature/), historical CO_2 concentrations from ref. [80] until 2014 and from NOAA GML from 2015 to 2020 (https://gml.noaa.gov/webdata/ccgg/trends/co2/co2_annmean_gl.txt), historical radiative forcing from non-CO_2 radiative agents from the RCP database, assuming RCP2.6 from 2005 to 2020 (https://tntcat.iiasa.ac.at/RcpDb/dsd?Action=htmlpage&page=welcome)[81–89], historical CO_2 fossil fuel and land-use change emissions from the Global Carbon Project[33], and historical CO_2-fe emissions from non-CO_2 forcing agents derived from the non-CO_2 radiative forcing from the RCP database.

The estimated warming in 2020, past cumulative CO_2-fe emissions, the remaining CO_2-fe emissions budgets to limit global warming to 1.5 °C and 2 °C and the estimated time when zero CO_2-fe emissions need to be reached based on this data lie within previous estimates. Previous estimates of anthropogenic warming are 1.0 ± 0.2 °C for 2017[2], 1.07 (0.8–1.3) °C for the period 2010–2019[29], and 1.20 °C for 2020[26]. In comparison, the AERA-derived warming estimates are 1.15 °C for 2017, 1.08 °C for 2010–2019, and 1.23 for 2020, in agreement with the three previous estimates. The resulting remaining CO_2-fe budget, when scaled to the remaining warming in 2020 (0.27 °C), was estimated to be 117–270 Pg C[7,21]. This estimation encompasses the REB estimate of 168 Pg C presented here.

Supplementary Methods

Additional information about the methods that are used throughout this study is made available as Supplementary Information. The Supplementary Information includes a detailed description of the AERA testing with Bern3D-LPX, the reduced form atmospheric chemistry model and the AERA robustness tests.

Data availability

The Bern3D-LPX model output is publicly available via SEANOE (https://doi.org/10.17882/90901)[90]. All other data are available in the main text or the supplementary materials.

Code availability

The AERA code is publicly available via https://github.com/Jete90/AERA[74].

References

74. Terhaar, J., Frölicher, T. L., Aschwanden, M. & Joos, F. Adaptive emission reduction approach (AERA). zenodo https://doi.org/10.5281/zenodo.7186275 (2022).
75. Millar, R. J., Nicholls, Z. R., Friedlingstein, P. & Allen, M. R. A modified impulse-response representation of the global near-surface air temperature and atmospheric concentration response to carbon dioxide emissions. *Atmos. Chem. Phys.* **17**, 7213–7228 (2017).

76. Palter, J. B., Frölicher, T. L., Paynter, D. & John, J. G. Climate, ocean circulation, and sea level changes under stabilization and overshoot pathways to 1.5 K warming. *Earth Syst. Dyn.* **9**, 817–828 (2018).
77. Koven, C. et al. Multi-century dynamics of the climate and carbon cycle under both high and net negative emissions scenarios. *Earth Syst. Dyn.* **13**, 885–909 (2022).
78. Zickfeld, K., MacDougall, A. H. & Matthews, H. D. On the proportionality between global temperature change and cumulative CO_2 emissions during periods of net negative CO_2 emissions. *Environ. Res. Lett.* **11**, 055006 (2016).
79. Tokarska, K. B., Zickfeld, K. & Rogelj, J. Path independence of carbon budgets when meeting a stringent global mean temperature target after an overshoot. *Earths Future* **7**, 1283–1295 (2019).
80. Meinshausen, M. et al. Historical greenhouse gas concentrations for climate modelling (CMIP6). *Geosci. Model Dev.* **10**, 2057–2116 (2017).
81. van Vuuren, D. P. et al. Stabilizing greenhouse gas concentrations at low levels: an assessment of reduction strategies and costs. *Clim. Change* **81**, 119–159 (2007).
82. Schultz, M. G. et al. Global wildland fire emissions from 1960 to 2000. *Glob. Biogeochem. Cycles* **22**, GB2002 (2008).
83. Mieville, A. et al. Emissions of gases and particles from biomass burning during the 20th century using satellite data and an historical reconstruction. *Atmos. Environ.* **44**, 1469–1477 (2010).
84. Eyring, V. et al. Transport impacts on atmosphere and climate: shipping. *Atmos. Environ.* **44**, 4735–4771 (2010).
85. Lee, D. S. et al. Aviation and global climate change in the 21st century. *Atmos. Environ.* **43**, 3520–3537 (2009).
86. Lamarque, J.-F. et al. Historical (1850–2000) gridded anthropogenic and biomass burning emissions of reactive gases and aerosols: methodology and application. *Atmos. Chem. Phys.* **10**, 7017–7039 (2010).
87. Hurtt, G. C. et al. Harmonization of land-use scenarios for the period 1500–2100: 600 years of global gridded annual land-use transitions, wood harvest, and resulting secondary lands. *Clim. Change* **109**, 117 (2011).
88. Smith, S. J., Pitcher, H. & Wigley, T. M. L. Global and regional anthropogenic sulfur dioxide emissions. *Glob. Planet. Change* **29**, 99–119 (2001).
89. Bond, T. C. et al. Historical emissions of black and organic carbon aerosol from energy-related combustion, 1850–2000. *Glob. Biogeochem. Cycles* **21**, GB2018 (2007).
90. Terhaar, J., Frölicher, T. L., Aschwanden, M. & Joos, F. Bern3D-LPX simulations with the the adaptive emission reduction approach (AERA). https://doi.org/10.17882/90901 (SEANOE, 2022).
91. Canadell, J. G. et al. in *IPCC Climate Change 2021: The Physical Science Basis* (eds Masson-Delmotte, V. P. et al.) Ch. 5 (Cambridge Univ. Press, 2021).

Acknowledgements

This work was funded by the European Union's Horizon 2020 research and innovation programme under grant agreement No 821003 (project 4C, Climate-Carbon Interactions in the Current Century) (J.T., T.L.F., F.J., P.F.) and grant agreement No 101003687 (project PROVIDE, Paris Agreement Overshooting) (T.L.F.), and by the Swiss National Science Foundation under grant PP00P2_198897 (T.L.F.) and grant #200020_200511 (F.J.). The work reflects only the authors' view; the European Commission and their executive agency are not responsible for any use that may be made of the information the work contains. We thank D. Guignet for initial analysis, S. Lienert and A. Jeltsch-Thömmes for help with Bern3D-LPX, and the 4C partners for helpful discussions.

Author contributions

J.T., T.L.F., F.J. and P.F. conceptualized the project. J.T., M.T.A., T.L.F. and F.J. developed the methodology. J.T. and M.T.A. developed the software. J.T. conducted the investigation. J.T., T.L.F. and F.J. performed visualization. T.L.F., F.J. and P.F. acquired funding. T.L.F. and F.J. administered the project. J.T. wrote the original draft. J.T., M.T.A., T.L.F., F.J. and P.F. reviewed and edited the manuscript.

Competing interests

The authors declare no competing interests.

Additional information

Extended data is available for this paper at https://doi.org/10.1038/s41558-022-01537-9.

Supplementary information The online version contains supplementary material available at https://doi.org/10.1038/s41558-022-01537-9.

Correspondence and requests for materials should be addressed to Jens Terhaar.

Peer review information *Nature Climate Change* thanks Piers Forster, Joeri Rogelj and Katsumasa Tanaka for their contribution to the peer review of this work.

https://doi.org/10.1038/s41558-022-01537-9

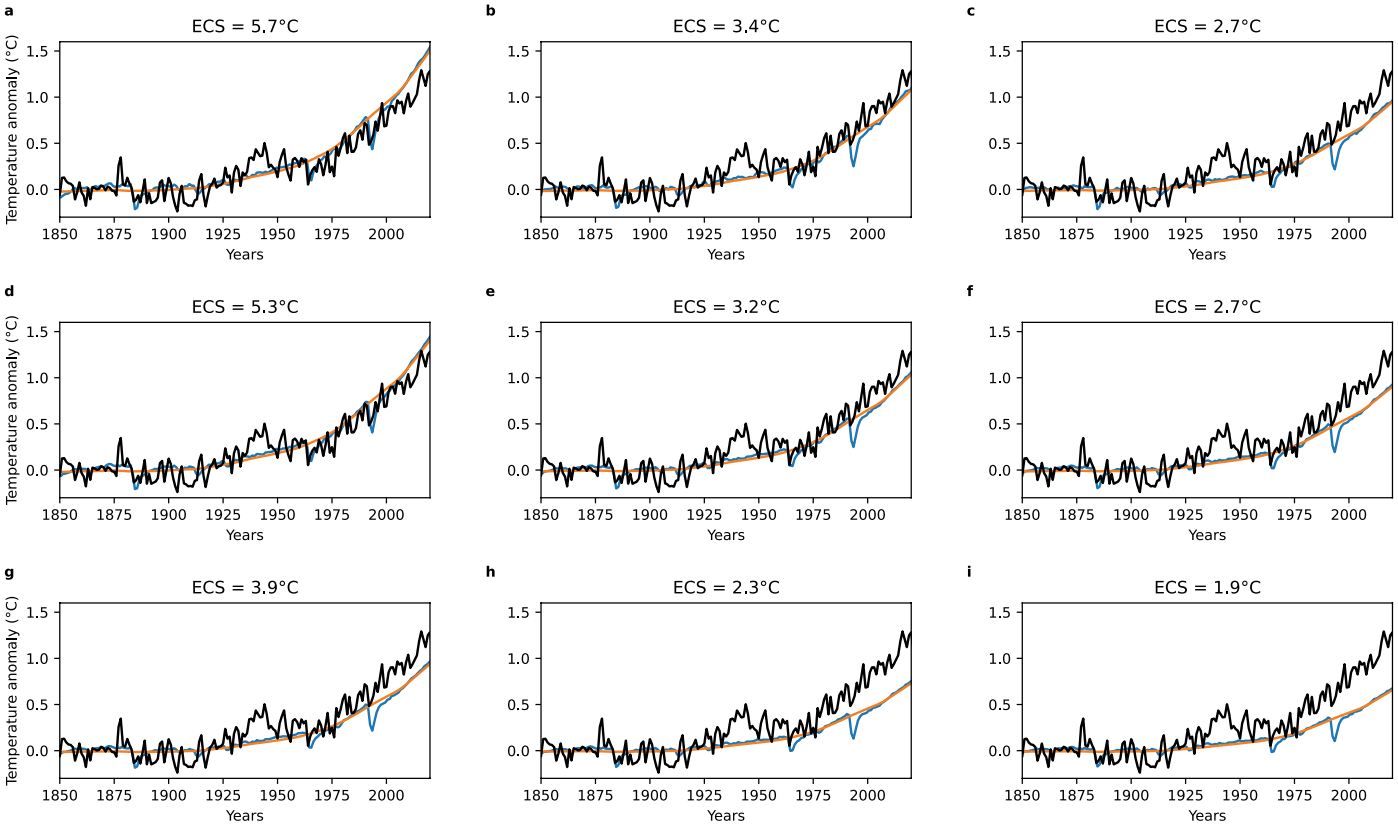

Extended Data Fig. 1 | Historical and simulated globally averaged surface atmospheric temperature anomaly with respect to 1850-1900 for different model configurations. (a-i) Global mean surface temperature (GMST) from 1850 to 2020 for 9 model configurations with varying ECS without the superimposed inter-annual variability. The blue lines show the simulated GMST, and the orange lines show the determined anthropogenic warming. The diapycnal diffusivity coefficients are 1×10^{-5}, 2×10^{-5} and 1×10^{-4} $m^2 s^{-1}$ (from top to bottom) and the different numbers for the internal Bern3D model parameter that accounts for climate feedbacks, which are not explicitly represented in the model, are 0.1, −0.3, and −0.7 W m^{-2} K^{-1} (from left to right). The HadCRUT5 observation-based GMST time-series is shown in black in all panels.

https://doi.org/10.1038/s41558-022-01537-9

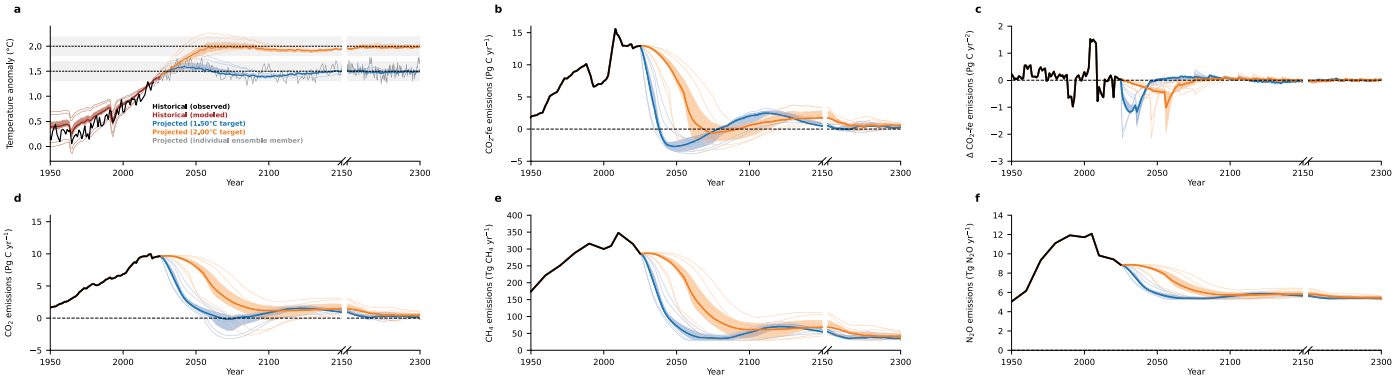

Extended Data Fig. 2 | Globally averaged surface atmospheric temperature anomaly with respect to 1850-1900, CO_2-fe emissions, their annual rate of change, as well as CO_2, CH_4, and N_2O emissions when applying the adaptive emission reduction approach every ten years. (a) Temperature anomalies with respect to 1850-1900, **(b)** CO_2-fe emissions, and **(c)** their annual rate of change if the AERA is applied every ten years starting in the year 2025 for the 1.5 °C target (blue) and the 2.0 °C target (orange). In addition, the AERA-calculated emission curves for **(d)** CO_2, **(e)** CH_4, and **(f)** N_2O are shown. CO_2 emission curves shown here do not include emissions from prescribed land-use change. As compared to Fig. 2 in the main text, here the AERA is applied every 10 years instead of every 5 years. The thick solid lines show the average of the 8 simulations with varying magnitude and timing of added inter-annual temperature variability of the Bern3D-LPX model configuration with an ECS of 3.2 °C, the thin solid lines show the same for the remaining 8 configurations covering ECS from 1.9 to 5.7 °C, and the shaded area shows the range of all configurations that fall within the likely range of ECS as defined by Sherwood et al.[24]. The grey shading in **(a)** indicates the uncertainty with which the anthropogenic warming can be determined (±0.2 °C)[26–29].

https://doi.org/10.1038/s41558-022-01537-9

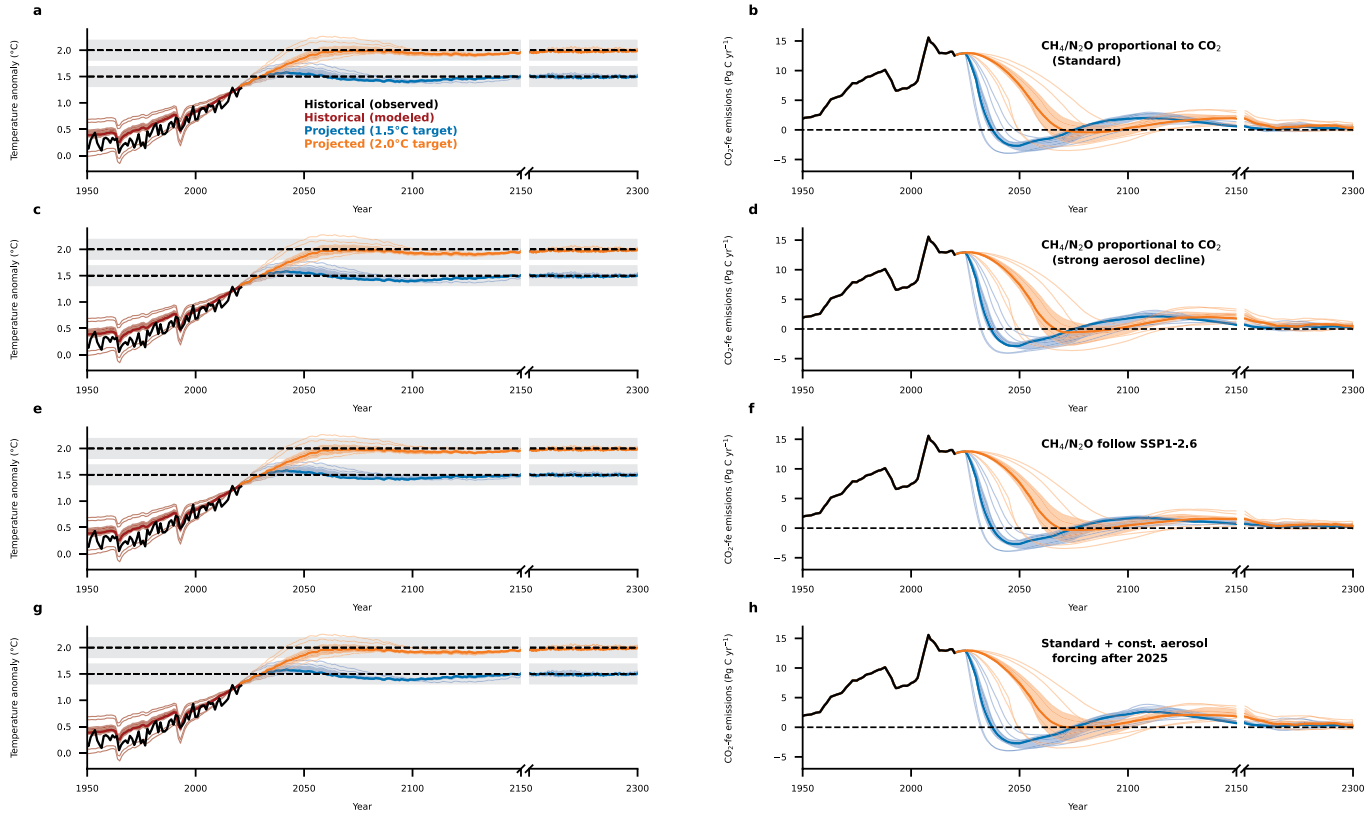

Extended Data Fig. 3 | Adaptive CO_2-fe emissions and resulting temperature anomaly for 1.5 °C and 2.0 °C target for different non-CO_2 GHG emissions and aerosol radiative forcing. **(a, c, e, g)** Temperature anomalies with respect to 1850-1900 and **(b, d, f, h)** corresponding CO_2-fe emissions if the AERA is applied every five years starting in the year 2025 for the 1.5 °C target (blue) and the 2.0 °C target (orange) for four different idealized cases: **(a, b)** aerosol radiative forcing decreases exponentially and CO_2, CH_4, and N_2O emissions evolve proportionally, **(c, d)** aerosol radiative forcing decreases according to the CO_2 emissions and CO_2, CH_4, and N_2O emissions evolve proportionally, **(e, f)** aerosol radiative forcing decreases exponentially but CH_4, and N_2O emissions follow prescribed trajectories from SSP1-2.6 after 2025 and only CO_2 evolves dynamically, and **(g, h)** aerosol radiative forcing remains constant after 2025 and CO_2, CH_4, and N_2O emissions evolve proportionally. CO_2 emission curves shown here do not include emissions from prescribed land-use change. The thick solid lines show the average of the 8 simulations with varying magnitude and timing of added inter-annual temperature variability of the Bern3D-LPX model configuration with an ECS of 3.2 °C and the shaded area shows the range of all configurations that fall within the likely range of ECS as defined by Sherwood et al.[24]. The grey shading in **(a, c, e, g)** indicates the uncertainty with which the anthropogenic warming can be determined (±0.2 °C)[26–29]. The corresponding CO_2, CH_4, and N_2O emissions and aerosol forcing for each simulated case are shown in Fig. 3.

https://doi.org/10.1038/s41558-022-01537-9

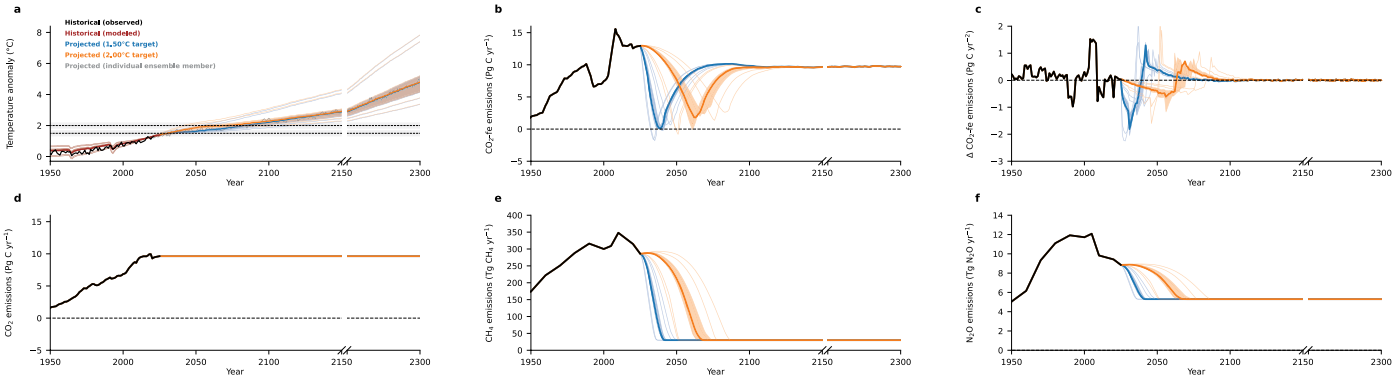

Extended Data Fig. 4 | Globally averaged surface atmospheric temperature anomaly with respect to 1850-1900, CO_2-fe emissions, their annual rate of change, as well as CO_2, CH_4, and N_2O emissions following the adaptive emission reduction approach when forcing CO_2 emissions to remain constant. (a) Temperature anomalies with respect to 1850-1900, **(b)** CO_2-fe emissions, and **(c)** their annual rate of change if the AERA is applied every five years starting in the year 2025 for the 1.5 °C target (blue) and the 2.0 °C target (orange). In addition, the AERA-calculated emission curves for **(d)** CO_2, **(e)** CH_4, and **(f)** N_2O are shown. As compared to Fig. 2 in the main text, here the CO_2 emissions are forced to remain constant while only CH_4, N_2O, VOC, NOx, and CO emissions evolve proportionally. The thick solid lines show the average of the 8 simulations with varying magnitude and timing of added inter-annual temperature variability of the Bern3D-LPX model configuration with an ECS of 3.2 °C, the thin solid lines show the same for the remaining 8 configurations covering ECS from 1.9 to 5.7 °C, and the shaded area shows the range of all configurations that fall within the likely range of ECS as defined by Sherwood et al.[24]. The grey shading in **(a)** indicates the uncertainty with which the anthropogenic warming can be determined (±0.2 °C)[26–29].

https://doi.org/10.1038/s41558-022-01537-9

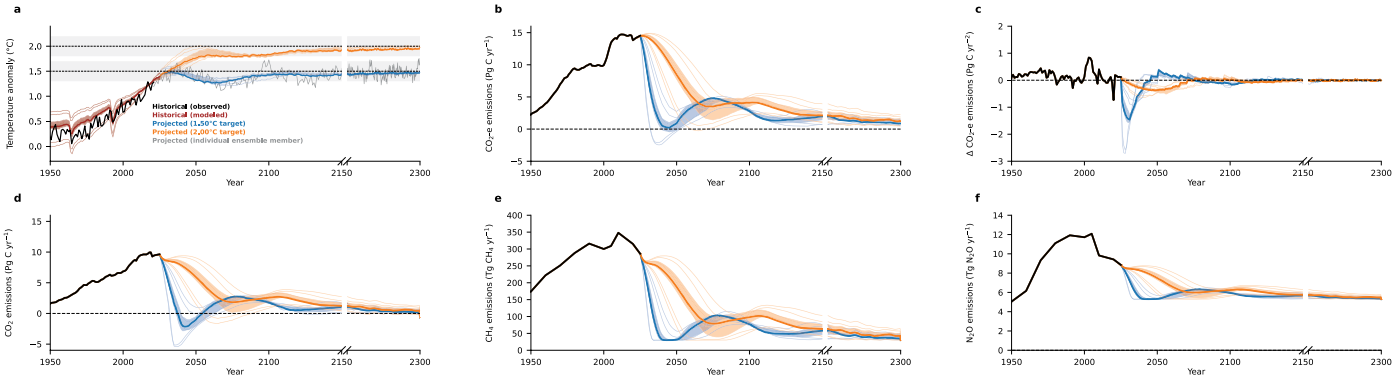

Extended Data Fig. 5 | Globally averaged surface atmospheric temperature anomaly with respect to 1850-1900, CO_2-e emissions, their annual rate of change, as well as CO_2, CH_4, and N_2O emissions following the adaptive emission reduction approach using GWP-100 instead of CO_2-fe to split CO_2-e emissions. (a) Temperature anomalies with respect to 1850-1900, **(b)** CO_2-e emissions, and **(c)** their annual rate of change if the AERA is applied every five years starting in the year 2025 for the 1.5 °C target (blue) and the 2.0 °C target (orange). In addition, the AERA-calculated emission curves for **(d)** CO_2, **(e)** CH_4, and **(f)** N_2O are shown. CO_2 emission curves shown here do not include emissions from prescribed land-use change. As compared to Fig. 2 in the main text, here the GWP-100 approach was used to calculate CO_2 equivalent emissions from CH_4 and N_2O emissions and the CO_2-fe emissions approach was applied to calculate CO_2 equivalent emissions from the remaining forcing agents. The thick solid lines show the average of the 8 simulations with varying magnitude and timing of added inter-annual temperature variability of the Bern3D-LPX model configuration with an ECS of 3.2 °C, the thin solid lines show the same for the remaining 8 configurations covering ECS from 1.9 to 5.7 °C, and the shaded area shows the range of all configurations that fall within the likely range of ECS as defined by Sherwood et al.[24]. The grey shading in **(a)** indicates the uncertainty with which the anthropogenic warming can be determined (±0.2 °C)[26–29].

https://doi.org/10.1038/s41558-022-01537-9

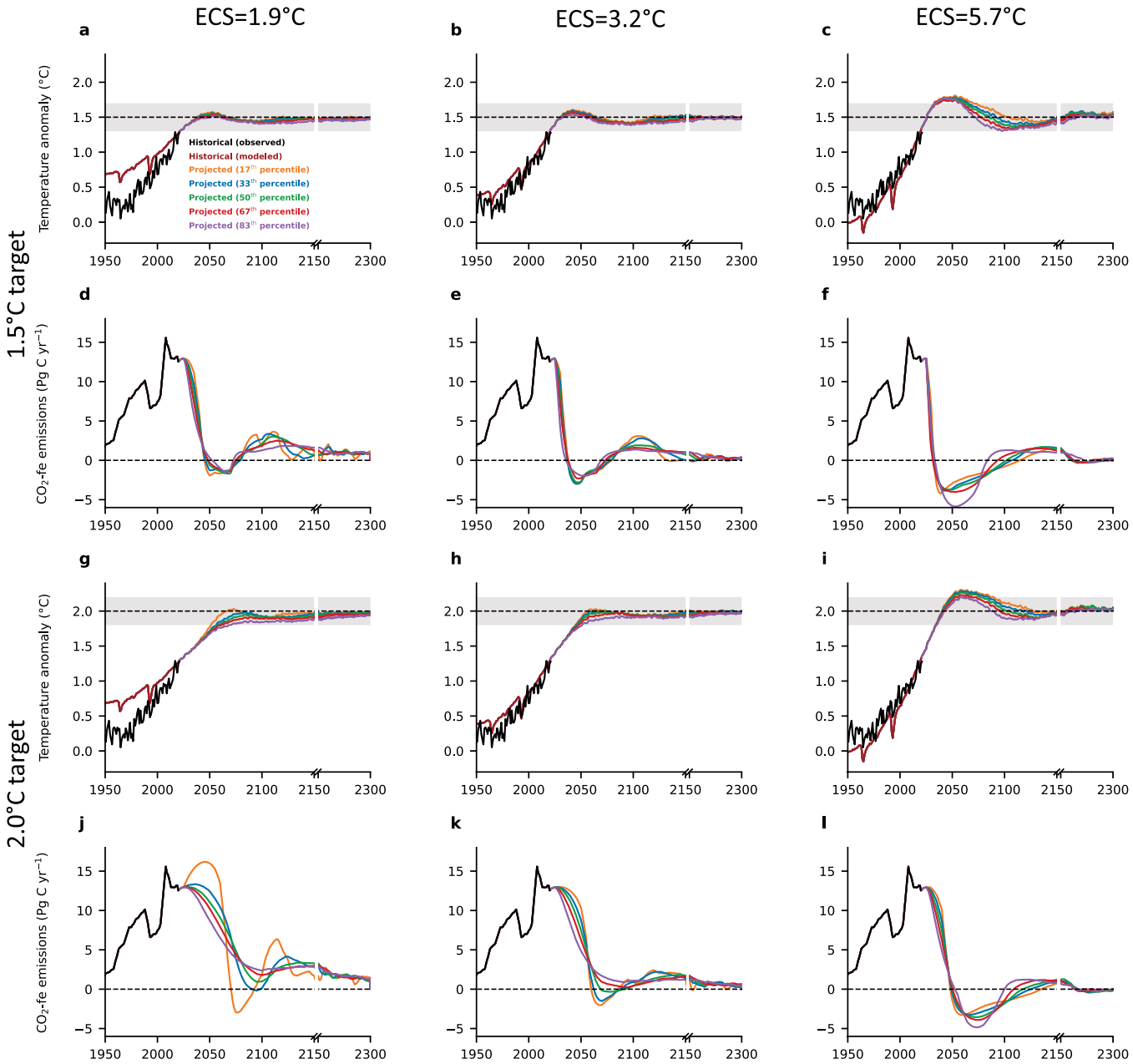

Extended Data Fig. 6 | Adaptive emissions and resulting temperature anomaly for 1.5 °C and 2.0 °C target with varying compliance. Temperature from 2020 to 2300 for three model configurations with varying ECS (1.9 °C **(a, d, g, j)**, 3.2 °C **(b, e, h, k)**, 5.7 °C **(c, f, i, l)**) averaged over four simulations each with different inter-annual variability for the **(a-c)** 1.5 °C and **(g-i)** 2.0 °C temperature target and **(d-f, j-l)** the respective CO_2-fe emission curves with different compliance, that is, at each stocktake the 17th (orange), 33rd (blue), 50th (green), 67th (red), or 83rd percentile (violet) was implemented. The percentiles are scaled at each stocktake based on the percentiles of the REB in 2020 from Table 5.8 of the IPCC AR6 WG1 report[91]. The grey shading in **(a, b, c, g, h, i)** indicates the uncertainty with which the anthropogenic warming can be determined (±0.2 °C)[26–29].

https://doi.org/10.1038/s41558-022-01537-9

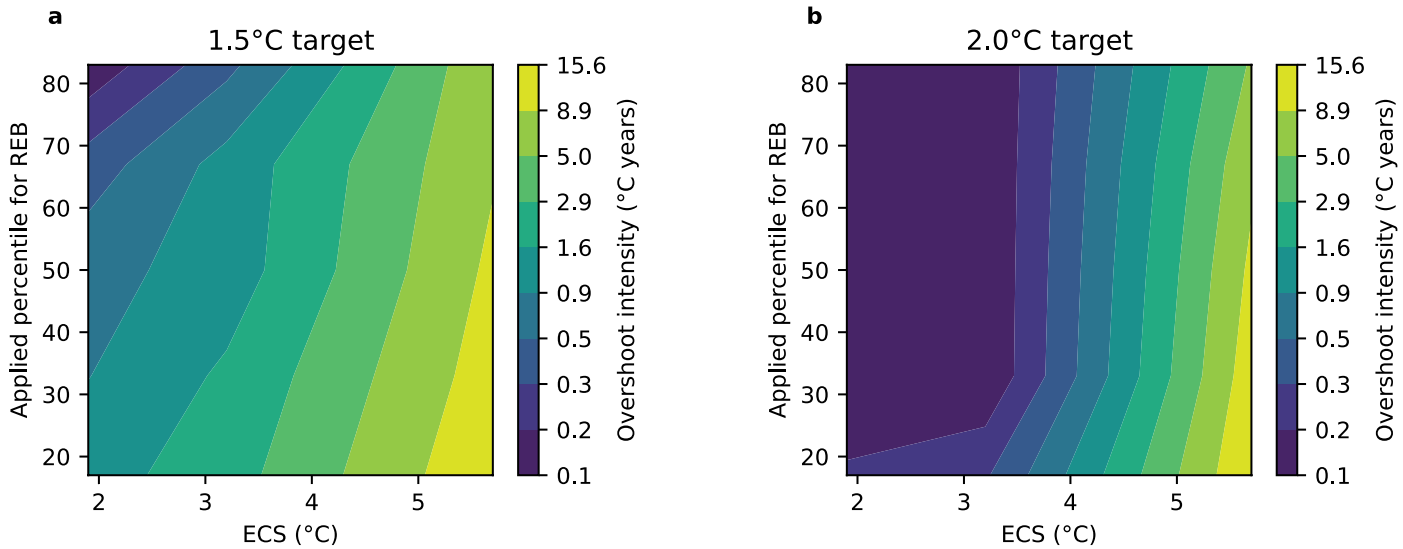

Extended Data Fig. 7 | Overshoot cumulative intensity for 1.5 °C and 2 °C temperature targets dependent on compliance and model configuration. Overshoot cumulative intensity (°C years), defined as the sum of the overshoot temperatures in each year, in dependence of model configuration (ECS from 1.9 °C to 5.7 °C) and the REB that was used in the AERA (17th, 33rd, 50th, 67th, and 83rd percentile) for (a) 1.5 °C and (b) 2 °C target.